A Genome-Wide Functional Investigation into the Roles of Receptor-Like Proteins in Arabidopsis[1][W][OA]

Guodong Wang[2], Ursula Ellendorff[2], Ben Kemp, John W. Mansfield, Alec Forsyth, Kathy Mitchell, Kubilay Bastas, Chun-Ming Liu, Alison Woods-Tör, Cyril Zipfel, Pierre J.G.M. de Wit, Jonathan D.G. Jones, Mahmut Tör, and Bart P.H.J. Thomma*

Plant Research International, B.V., Business Unit of Bioscience, 6700 AA Wageningen, The Netherlands (G.W., C.M.L.); Laboratory of Phytopathology, Wageningen University, 6709 PD Wageningen, The Netherlands (U.E., P.J.G.M.W., B.P.H.J.T.); Warwick HRI, University of Warwick, Wellesbourne, Warwick CV35 9EF, United Kingdom (B.K., K.B., A.W.-T., M.T.); Imperial College London, Division of Biology, Wye Campus, Wye, Ashford, Kent TN25 5AH, United Kingdom (J.W.M., A.F., K.M.); Center for Signal Transduction and Metabolomics, Institute of Botany, Chinese Academy of Sciences, Beijing 100093, China (C.-M.L.); and Sainsbury Laboratory, John Innes Centre, Norwich Research Park, Norwich NR4 7UH, United Kingdom (C.Z., J.D.G.J.)

Receptor-like proteins (RLPs) are cell surface receptors that typically consist of an extracellular leucine-rich repeat domain, a transmembrane domain, and a short cytoplasmatic tail. In several plant species, RLPs have been found to play a role in disease resistance, such as the tomato (*Solanum lycopersicum*) Cf and Ve proteins and the apple (*Malus domestica*) HcrVf2 protein that mediate resistance against the fungal pathogens *Cladosporium fulvum*, *Verticillium* spp., and *Venturia inaequalis*, respectively. In addition, RLPs play a role in plant development; Arabidopsis (*Arabidopsis thaliana*) TOO MANY MOUTHS (TMM) regulates stomatal distribution, while Arabidopsis CLAVATA2 (CLV2) and its functional maize (*Zea mays*) ortholog FASCINATED EAR2 regulate meristem maintenance. In total, 57 *RLP* genes have been identified in the Arabidopsis genome and a genome-wide collection of T-DNA insertion lines was assembled. This collection was functionally analyzed with respect to plant growth and development and sensitivity to various stress responses, including susceptibility toward pathogens. A number of novel developmental phenotypes were revealed for our *CLV2* and *TMM* insertion mutants. In addition, one *AtRLP* gene was found to mediate abscisic acid sensitivity and another *AtRLP* gene was found to influence nonhost resistance toward *Pseudomonas syringae* pv *phaseolicola*. This genome-wide collection of Arabidopsis *RLP* gene T-DNA insertion mutants provides a tool for future investigations into the biological roles of RLPs.

For decades, it was thought that the communication between plant cells occurs through the cell wall-spanning cytoplasmic bridges called plasmodesmata. However, since the identification of the first plant cell surface receptor (Walker and Zhang, 1990), it has been known that, similar to other multicellular organisms, plants can perceive extracellular signals at the plasma membrane. Since then, many plant cell surface receptors have been found to play key roles in very diverse processes ranging from growth and development, in which they perceive endogenous self signals, to recognition of other organisms, in which they perceive exogenous nonself signals (Diévart and Clark, 2004).

A common structural element of many plant cell surface receptors is the extracellular Leu-rich repeat (eLRR) domain that is generally thought to mediate ligand perception (Kobe and Kajava, 2001; Kinoshita et al., 2005). These eLRRs are composed of 23 to 25 amino acids with the conserved consensus sequence LxxLxxLxLxxNxLt/sgxIpxxLG (Jones and Jones, 1997). The largest group of eLRR-containing cell surface receptors is formed by the receptor-like kinases (RLKs) that are composed of an eLRR domain, a single-pass transmembrane domain, and a cytoplasmic kinase domain, with over 200 representatives in the Arabidopsis (*Arabidopsis thaliana*) genome (Shiu and Bleecker, 2003). The second largest group of eLRR-containing cell surface receptors is formed by the receptor-like proteins (RLPs) that differ from RLKs in that they lack the cytoplasmic kinase domain and only have a short cytoplasmic tail that lacks obvious motifs for intracellular

[1] This work was supported by the Dutch Graduate School of Experimental Plant Sciences, by the Research Council for Earth and Life Sciences of the Netherlands Organization for Scientific Research (VIDI grant to B.P.H.J.T.), by the UK Biotechnology and Biological Sciences Research Council (to J.W.M., B.K., A.W.-T., and M.T.), by the Gatsby Charitable Foundation (to C.Z. and J.D.G.J.), and by a postdoctoral long-term fellowship from the European Molecular Biology Organization (to C.Z.).

[2] These authors contributed equally to the article.

* Corresponding author; e-mail bart.thomma@wur.nl.

The authors responsible for distribution of materials integral to the findings presented in this article in accordance with the policy described in the Instructions for Authors (www.plantphysiol.org) are: Bart P.H.J. Thomma (bart.thomma@wur.nl) and Mahmut Tör (mahmut.tor@warwick.ac.uk).

[W] The online version of this article contains Web-only data.

[OA] Open Access articles can be viewed online without a subscription.

www.plantphysiol.org/cgi/doi/10.1104/pp.108.119487

signaling except for the putative endocytosis motif found in some members (Joosten and de Wit, 1999; Kruijt et al., 2005). Typically, the amino acid sequence of RLPs has been divided into the conserved domains A through G with a putative signal peptide (A), a Cys-rich domain (B), the LRR domain (C), a spacer (D), an acidic domain (E), the transmembrane domain (F), and a short cytoplasmic region (G). Furthermore, the LRR-containing C domain is subdivided into three domains in which the non-LRR island C2 domain interrupts the C1 and C3 LRR regions (Jones and Jones, 1997).

Recently, considerable advances have been made in our understanding of the role and function of RLKs and how they relay extracellular signals to initiate an intracellular response (Nürnberger and Kemmerling, 2006; Li and Jin, 2007). By contrast, very little is known about RLP signaling (Fritz-Laylin et al., 2005; Kruijt et al., 2005). The first *RLP* gene identified was tomato (*Solanum lycopersicum*) *Cf-9* that mediates resistance against strains of the leaf mold fungus *Cladosporium fulvum* that carry the avirulence gene *Avr9* (Jones et al., 1994). *C. fulvum* is a biotrophic pathogen that is characterized by strictly apoplastic growth (Thomma et al., 2005). To date, several *Cf* resistance genes have been cloned from tomato that all to belong to the *RLP* gene family (Dixon et al., 1996, 1998; Thomas et al., 1997; Takken et al., 1999). In addition to *Cf* genes, the *RLP* gene family in tomato comprises two *Ve* genes that have been reported to provide resistance against vascular wilt pathogens of the genus *Verticillium* (Kawchuk et al., 2001) that, like *C. fulvum*, grow extracellularly without penetrating plant cells (Fradin and Thomma, 2006). Finally, the tomato *RLP* family comprises two *LeEIX* genes that encode receptors for the ethylene-inducible xylanase produced by extracellularly growing *Trichoderma* biocontrol fungi (Ron and Avni, 2004).

In addition to tomato, RLPs have been implicated in disease resistance in other plant species (Kruijt et al., 2005). Apple (*Malus domestica*) *HcrVf-2* confers resistance to the apple scab fungus *Venturia inaequalis* (Belfanti et al., 2004). Furthermore, an Arabidopsis chitin-inducible *RLP* gene has been implicated in resistance against the powdery mildew pathogen *Erysiphe cichoracearum* (Ramonell et al., 2005).

RLPs also play significant roles in plant development. For example, Arabidopsis CLAVATA2 (CLV2) was found to be crucial for maintaining a balanced meristematic stem cell population and is required for the accumulation and stability of CLV1, which is an RLK (Jeong et al., 1999). It has been proposed that CLV1 and CLV2 undergo a physical interaction to form a heterodimer to act as receptor for the predicted extracellular peptide ligand CLV3 (Trotochaud et al., 1999; Rojo et al., 2002; Ogawa et al., 2008). Upon ligand perception by the ectodomain (Ogawa et al., 2008), the kinase domain of CLV1 is thought to be activated to initiate the downstream signaling that is required to maintain the stem cell population (Rojo et al., 2002; Diévart and Clark, 2004). In maize (*Zea mays*), an ortholog of the *CLV2* gene has been identified as *FASCINATED EAR2* (Taguchi-Shiobara et al., 2001). Furthermore, the RLK thick tassel dwarf1 has been identified as a CLV1 ortholog, suggesting that the CLAVATA signaling pathway is conserved between monocots and dicots (Bommert et al., 2005). Another *RLP* gene, *TOO MANY MOUTHS* (*TMM*), is involved in plant development in Arabidopsis and regulates stomatal distribution across the epidermis (Nadeau and Sack, 2002). Although a physical interaction between TMM and any other RLP or RLK has not been established, TMM was found to negatively regulate three RLKs of the *ERECTA* family (Shpak et al., 2005).

Previously, in the Arabidopsis genome, 56 putative *RLP* genes (*AtRLP*s) were identified that are assembled at 33 loci (Fritz-Laylin et al., 2005). So far, a function has been assigned only to the three *AtRLP* genes described above (Jeong et al., 1999; Nadeau and Sack, 2002; Ramonell et al., 2005), implicating that the other RLPs are orphan proteins. In the complete genome sequence of the monocot plant rice (*Oryza sativa*), 90 *RLP* genes have been identified (Fritz-Laylin et al., 2005). Genes involved in plant development are presumably under evolutionary pressure to maintain a specific function that reduces sequence drift across orthologs, while disease resistance genes are under strong diversifying selection to produce highly divergent sequences with distinct recognition capacities (Fritz-Laylin et al., 2005). Based on the sequence comparison between Arabidopsis and rice *RLP* genes, and building on the hypothesis that developmental genes are less likely to be duplicated and undergo diversifying selection than are disease resistance genes (Leister, 2004), nine *AtRLP* genes were proposed as putative developmental orthologous genes, while the remaining *AtRLP* genes were proposed to be candidate disease resistance genes (Fritz-Laylin et al., 2005). In this article, we report on the assembly and functional analysis of a genome-wide collection of *AtRLP* family T-DNA knockout lines. This collection has been screened for altered phenotypes in growth and development but also alterations in response to pathogen challenge. Our analysis has revealed novel phenotypes linked with mutations in the well-studied AtRLPs TMM and CLV2. Furthermore, one *AtRLP* gene is found to play a role in abscisic acid (ABA) signaling, a process in which RLP activity has not been implicated previously. Remarkably, despite an extensive list of pathogens tested, including adapted and nonadapted pathogens of Arabidopsis, we have been able to identify only one *AtRLP* gene with a role in basal nonhost resistance against the nonadapted bacterial pathogen *Pseudomonas syringae* pv *phaseolicola* (*Psp*). The described *AtRLP* T-DNA collection is a valuable source for future investigations into the biological roles of RLPs.

RESULTS

AtRLP Gene Structure and AtRLP Protein Analysis

At the onset of this project, a bioinformatic analysis to investigate the structure of all the *AtRLP* genes was

undertaken. To this end, BLAST searches were performed on the Arabidopsis genome sequence using the predicted protein sequences of the previously characterized RLPs CLV2, TMM, and Cf-9 as queries. The set of Arabidopsis genes obtained in this way was further analyzed for the presence of a signal peptide, eLRRs, a transmembrane domain, and a short cytoplasmic tail lacking kinase motifs in the predicted protein. Although a previously published study has identified in total 56 *AtRLP* genes (Fritz-Laylin et al., 2005), our analysis revealed a set of 57 putative *AtRLP* genes (Table I). All 57 *AtRLP* genes were assigned AtRLP numbers in consecutive order according to their gene numbers along the Arabidopsis genome (Table I). The additional *AtRLP* gene identified here, denoted as *AtRLP5*, corresponds to At1g34290, and, although it carries only two eLRRs, the predicted protein complies with the canonical RLP domain composition.

Pairwise amino acid sequence comparison revealed that AtRLPs display low overall sequence identity, with only 10 pairwise combinations that share over 70% identity (Supplemental Table S1). Of these, the proteins encoded by the neighboring genes *AtRLP41* and *AtRLP42* share the highest level of identity (86%). Furthermore, both proteins are highly similar to AtRLP39 (85% and 82% identity, respectively), and the corresponding genes reside in close proximity to each other, suggesting recent gene multiplication. Two other AtRLP proteins, AtRLP44 and AtRLP57, are found to be similar in length and domain composition, sharing 80% identity (Fig. 1; Supplemental Table S1), although the genes that encode these proteins are located on different chromosomes. To further assess the structures of *AtRLP* genes, the exon boundaries and corresponding flanking intron sequences were determined. While only 21% of the genes in the Arabidopsis genome are composed of a single exon (Arabidopsis Genome Initiative, 2000), 37 of the 57 (65%) AtRLP-encoding genes were found to contain a single exon (Fig. 1). Interestingly, within the group of genes that contain multiple exons, *AtRLP9*, *AtRLP14*, *AtRLP15*, *AtRLP21*, and *AtRLP56* have introns at similar positions in the genes (Fig. 1). Similarly, the introns of *AtRLP19*, *AtRLP33*, and *AtRLP34* are also localized at comparable positions (Fig. 1). Furthermore, all the *AtRLP* genes that contain multiple exons cluster in a phylogenetic tree (Fig. 1).

Next, the domain composition was analyzed for all predicted AtRLP proteins. As has been noted previously (Fritz-Laylin et al., 2005), the AtRLPs exhibit great variation at the sequence level and also in the numbers of eLRRs (Fig. 1). The predicted sizes of the AtRLPs range from 218 amino acids (AtRLP25) to 1,784 amino acids (AtRLP9), whereas the eLRRs vary in number from two (AtRLP5) to 49 (AtRLP9; Fig. 1). Of the 57 AtRLPs, 18 are predicted to contain two transmembrane domains, one at the N terminus and one at the C terminus, although it is presently unclear whether the N terminal transmembrane domain indeed functions as such. Furthermore, it has previously been noted that not all RLPs contain an island domain (C2) within the eLRR region, with TMM as an example (Nadeau and Sack, 2002). Of the 57 AtRLPs, 45 are predicted to contain a C2 island domain nested in between two eLRR blocks (C1 and C3). Remarkably, in 42 of those RLPs, the island domain is followed by a C3 domain that contains exactly four eLRRs (Fig. 1). This distinct domain organization has not only been observed for some functionally characterized RLPs but also for some RLKs (Jones et al., 1994; Song et al., 1995; Clark et al., 1997; Li and Chory, 1997; Jeong et al., 1999; Gómez-Gómez and Boller, 2000; Taguchi-Shiobara et al., 2001). For all *AtRLP* genes, corresponding cDNA sequences, EST sequences, Massively Parallel Signature Sequencing data, and/or microarray data are deposited in public databases, demonstrating that all 57 *AtRLP* genes are actively transcribed (Supplemental Figs. S1 and S2).

Assembly of a Genome-Wide Collection of *AtRLP* Gene T-DNA Insertion Mutants

To identify putative T-DNA insertion lines for all the *AtRLP* genes, we queried the T-DNA Express database of the SALK Institute Genome Analysis Laboratory (SIGnAL; http://signal.salk.edu). Because often several different insertion lines could be identified for each *AtRLP* gene, insertion lines were selected based on the position of the T-DNA insertion within the coding sequence to enhance the likelihood of successful disruption of gene function. Preferably, T-DNA insertion lines of the Columbia (Col-0) ecotype were selected with exon insertions (Table I). However, if not available, lines with predicted intron (one line), promoter (11 lines), or terminator (four lines) insertions were chosen. For the 57 *AtRLP* genes, 89 T-DNA insertion lines were selected (Table I) that were evaluated for presence of the predicted T-DNA insertion using PCR (Supplemental Table S2). Ten lines did not have the predicted insertion, whereas 79 were confirmed to carry a T-DNA insertion in the gene of interest and for which homozygosity of the T-DNA insert was pursued. For two T-DNA insertion lines, FLAG_524A03 and SALK_012745 with an insertion in *AtRLP19* and *AtRLP37*, respectively, only heterozygous insertion lines were obtained, suggesting that homozygosity of these T-DNA mutations caused embryonic lethality. However, subsequent segregation and complementation analysis could not confirm embryo lethality caused by T-DNA homozygosity in these lines, and they were not used for further analysis. Although we were able to identify another T-DNA insertion line for *AtRLP37* that was carried to homozygosity (Table I), unfortunately, no alternative T-DNA insertion line was available for *AtRLP19*. Overall, in the complete collection of 77 homozygous *AtRLP* T-DNA insertion lines, at least one line was obtained for 56 of the 57 *AtRLP* genes, while for 19 *AtRLP* genes multiple mutants were identified (Table I).

Table I. *List of the AtRLP genes and corresponding T-DNA insertion lines used in this study*

Gene Name[a]	AGI Code	T-DNA Line Ordered	Mutant Name
AtRLP1	at1g07390	SALK_059920[b]	*Atrlp1-1*
		SALK_116923	*Atrlp1-2*
AtRLP2	at1g17240	SALK_049366[c]	*Atrlp2-1*
AtRLP3	at1g17250	SALK_051677	*Atrlp3-1*
		SAIL_204_D01[d]	*Atrlp3-2*
AtRLP4	at1g28340	SALK_039264[e]	*Atrlp4-1*
AtRLP5	at1g34290	SALK_112291	*Atrlp5-1*
AtRLP6	at1g45616	SALK_080898	*Atrlp6-1*
		SAIL_84_E01[d]	*Atrlp6-2*
		SALK_020071[f]	
AtRLP7	at1g47890	SALK_030269	*Atrlp7-1*
AtRLP8	at1g54480	SM_3_38632	*Atrlp8-1*
		SM_3_20200	*Atrlp8-2*
AtRLP9	at1g58190	SALK_061979	*Atrlp9-1*
		SALK_023419	*Atrlp9-2*
AtRLP10	at1g65380	GABI_686A09	*Atrlp10-1*
(*CLV2*)		clv2-3 (EMS)[g]	*clv2-3*
AtRLP11	at1g71390	SALK_013218	*Atrlp11-1*
AtRLP12	at1g71400	SALK_151456	*Atrlp12-1*
AtRLP13	at1g74170	SALK_020984	*Atrlp13-1*
AtRLP14	at1g74180	SAIL_513_A08[d]	*Atrlp14-1*
AtRLP15	at1g74190	SALK_041143	*Atrlp15-1*
		GABI_077G01[f]	
AtRLP16	at1g74200	SALK_032150	*Atrlp16-1*
AtRLP17	at1g80080	FLAG_014F03[d]	*Atrlp17-1*
(*TMM*)		*tmm-1* (EMS)[h]	*tmm-1*
		SAIL_165_F02[d,f]	
AtRLP18	at2g15040	SAIL_400_H02[d]	*Atrlp18-1*
AtRLP19	at2g15080	FLAG_524A03[d,i,j]	*Atrlp19-1*
AtRLP20	at2g25440	SALK_130147[c]	*Atrlp20-1*
AtRLP21	at2g25470	SAIL_693_F05	*Atrlp21-1*
		SALK_133403[f]	
AtRLP22	at2g32660	SALK_125231	*Atrlp22-1*
AtRLP23	at2g32680	SALK_034225	*Atrlp23-1*
AtRLP24	at2g33020	SALK_046236	*Atrlp24-1*
AtRLP25	at2g33030	SALK_048434[i]	*Atrlp25-1*
AtRLP26	at2g33050	SALK_104127[c]	*Atrlp26-1*
		SALK_026997[f]	
AtRLP27	at2g33060	SALK_029443	*Atrlp27-1*
AtRLP28	at2g33080	SM_3_1740	*Atrlp28-1*
AtRLP29	at2g42800	SALK_022220	*Atrlp29-1*
AtRLP30	at3g05360	SALK_122528	*Atrlp30-1*
		SALK_008911	*Atrlp30-2*
		SALK_122536	*Atrlp30-3*
		SALK_145342	*Atrlp30-4*
AtRLP31	at3g05370	SALK_058586	*Atrlp31-1*
		SALK_094160	*Atrlp31-2*
AtRLP32	at3g05650	FLAG_588C11[d]	*Atrlp32-1*
AtRLP33	at3g05660	FLAG_048F06[d]	*Atrlp33-1*
		SALK_087631	*Atrlp33-2*
		SALK_085252	*Atrlp33-3*
AtRLP34	at3g11010	SALK_067155	*Atrlp34-1*
		SALK_085506[f]	
AtRLP35	at3g11080	SALK_096171	*Atrlp35-1*
		SALK_016143	*Atrlp35-2*
AtRLP36	at3g23010	SALK_086147	*Atrlp36-1*
AtRLP37	at3g23110	SALK_041785	*Atrlp37-1*
		SALK_012745[j]	*Atrlp37-2*
AtRLP38	at3g23120	SALK_017819	*Atrlp38-1*
		GT_5_105490[d,f]	
AtRLP39	at3g24900	SALK_126505	*Atrlp39-1*
		SALK_126504[f]	
AtRLP40	at3g24982	GABI_564D03	*Atrlp40-1*
AtRLP41	at3g25010	SALK_024020	*Atrlp41-1*
		SM_3_20242	*Atrlp41-2*
		SM_3_38956	*Atrlp41-3*
AtRLP42	at3g25020	SALK_080324[b]	*Atrlp42-1*
		SALK_094190[b]	*Atrlp42-2*
AtRLP43	at3g28890	SALK_041685	*Atrlp43-1*
AtRLP44	at3g49750	SALK_097350[i]	*Atrlp44-1*
		SALK_045246[c]	*ATrlp44-2*
AtRLP45	at3g53240	GABI_620G05	*Atrlp45-1*
		FLAG_339H12[c,d]	*Atrlp45-2*
AtRLP46	at4g04220	SALK_048207[i]	*Atrlp46-1*
		SAIL_15_A02[d,f]	
AtRLP47	at4g13810	SALK_105921	*Atrlp47-1*
AtRLP48	at4g13880	SALK_036842	*Atrlp48-1*
AtRLP49	at4g13900	SALK_067372	*Atrlp49-1*
		SALK_116910	*Atrlp49-2*
AtRLP50	at4g13920	SALK_070876[i]	*Atrlp50-1*
AtRLP51	at4g18760	SALK_143038	*Atrlp51-1*
		SAIL_740_C06[i]	*Atrlp51-2*
AtRLP52	at5g25910	SALK_107922	*Atrlp52-1*
		SALK_054976[f]	
AtRLP53	at5g27060	SALK_124008	*Atrlp53-1*
AtRLP54	at5g40170	SAIL_306_E09[d]	*Atrlp54-1*
AtRLP55	at5g45770	SALK_139161[b]	*Atrlp55-1*
		SALK_076590	*Atrlp55-2*
AtRLP56	at5g49290	SALK_129306	*Atrlp56-1*
		SALK_010565	*Atrlp56-2*
AtRLP57	at5g65830	SALK_077716	*Atrlp57-1*

[a]In chronological order along the five Arabidopsis chromosomes. [b]T-DNA insertion site within 300 nucleotides downstream of the open reading frame. [c]T-DNA insertion site between 300 and 1,000 nucleotides upstream of the open reading frame. [d]SAIL-lines are in CS8846, FLAG-lines in WS-2 and GT-line is in L*er* background. [e]T-DNA insertion site within an intron. [f]T-DNA insertion site could not be confirmed by PCR; no homozygous T-DNA insertion line was obtained. [g]EMS mutant *clv2-3* (Jeong et al., 1999). [h]EMS mutant *tmm-1* (Nadeau and Sack, 2002). [i]T-DNA insertion site within 300 nucleotides upstream of the open reading frame. [j]No homozygous line for the T-DNA insertion was be obtained.

Phenotypic Alterations in Growth and Development of *AtRLP* Gene T-DNA Insertion Mutants

We examined the phenotypes of the complete collection of homozygous T-DNA insertion lines with respect to various characteristics related to plant growth and development. The T-DNA lines were examined for root development, rosette growth, inflorescence emergence, and the development and appearance of flowers and seed. In addition, stomatal patterning across the cotyledons and leaves, formation of the leaf cuticle, and the leaf vascular patterns were analyzed. Two *AtRLP* genes, *CLV2* (*AtRLP10*) and *TMM* (*AtRLP17*), have previously been implicated in plant development (Jeong et al., 1999; Nadeau and Sack, 2002). Our analysis showed that the T-DNA

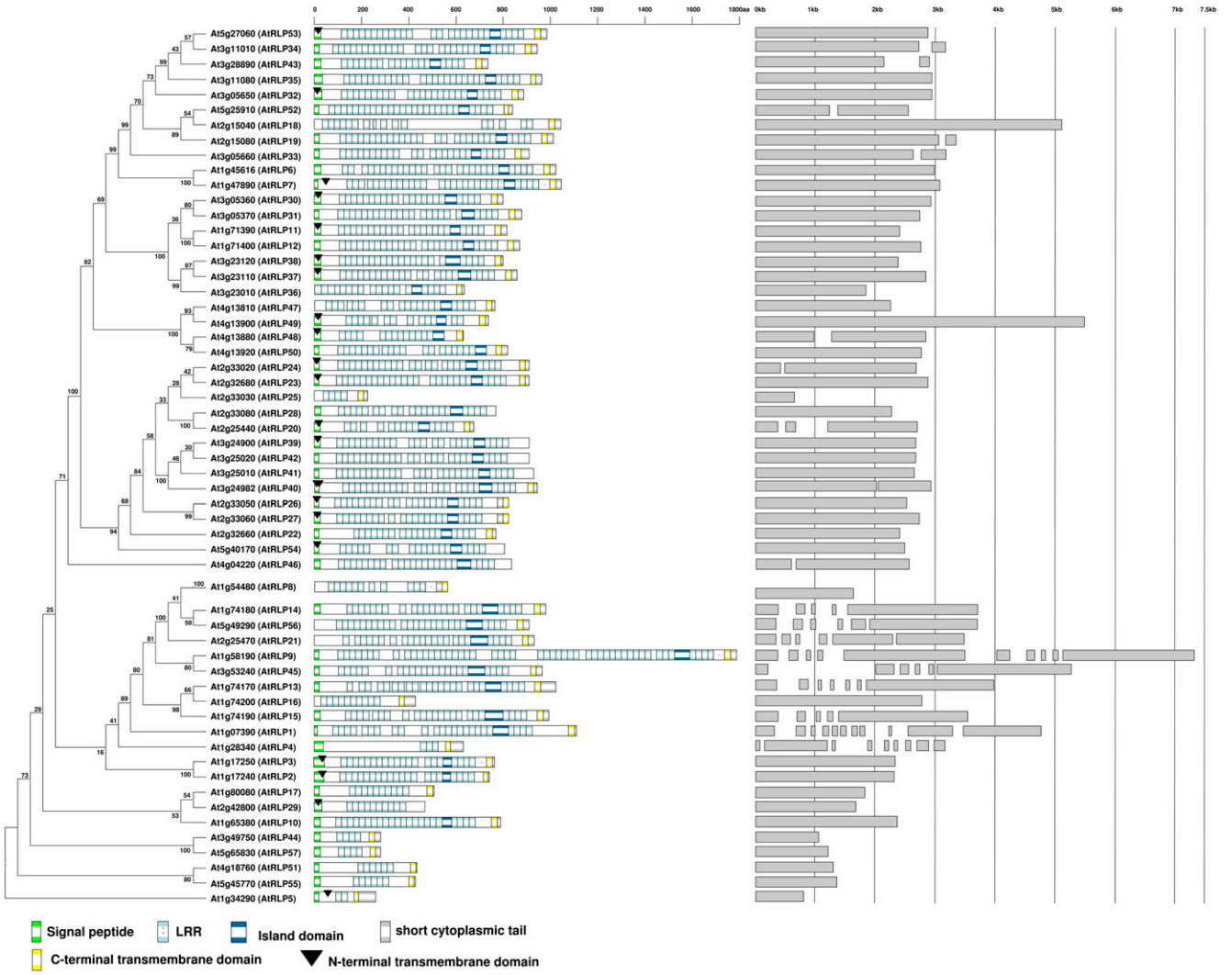

Figure 1. A phylogenetic view of AtRLP protein domain configurations and the corresponding *RLP* gene structures as shown by exon/intron boundaries. Left, Phylogenetic tree of the AtRLP family that also includes CLV2 (AtRLP10) and TMM (AtRLP17). The tree was generated from the alignment of C3-F domains of all AtRLPs with 100 bootstrap replicates as indicated on the branch of the tree. The AGI code and *AtRLP* gene number are indicated on the left. Genes are organized according to the order along the chromosomes. Middle, Domain organizations as predicted by SMART/Pfam. Each colored box represents a domain as indicated. The arrowhead shows the putative N-terminal transmembrane domain. The open box indicates an amino acid fragment not showing any significant motif or domain. Right, *RLP* gene structure presented by gray boxes for exons and spaces for the introns.

insertion lines *Atrlp10-1* and *Atrlp17-1* for the *CLV2* and the *TMM* gene, respectively, displayed phenotypes that have previously been reported for a number of mutants in these genes (Yang and Sack, 1995; Kayes and Clark, 1998; Jeong et al., 1999; Nadeau and Sack, 2002). Similar to the ethyl methanesulfonate (EMS) mutant *tmm-1*, the stomata of the knockout allele *Atrlp17-1* that carries a T-DNA in the ATG start codon of the coding sequence were found to cluster across the leaf epidermis (Fig. 2, A–D and J). Complementation of *Atrlp17-1* with the wild-type *TMM* allele resulted in disappearance of the stomatal clustering phenotype (Fig. 2E), showing that *Atrlp17-1* is a true *TMM* mutant allele. In addition, as expected, the *Atrlp10-1* mutant with a knockout in the *CLV2* gene displayed enlarged shoot meristem (Fig. 3, D and E) and alterations in the development of the gynoecia, flowers, carpels, pedicels, and stamens (data not shown). Like other *CLV2* mutants, the *Atrlp10-1* mutant fails to respond to in vitro treatment with a synthetic peptide that corresponds to the conserved CLE motif that is present in the CLV3-like peptide ligands (Fig. 3H; Fiers et al., 2005). However, while the previously described *CLV2* mutants (*clv2-1* to *clv2-5*) generally have four carpels (Kayes and Clark, 1998), *Atrlp10-1* shows only a mild carpel phenotype with 2.6 carpels on average (Fig. 3N).

Interestingly, despite the relatively weak carpel phenotype, *Atrlp10-1* exhibits a number of phenotypes that have not previously been reported for any of the

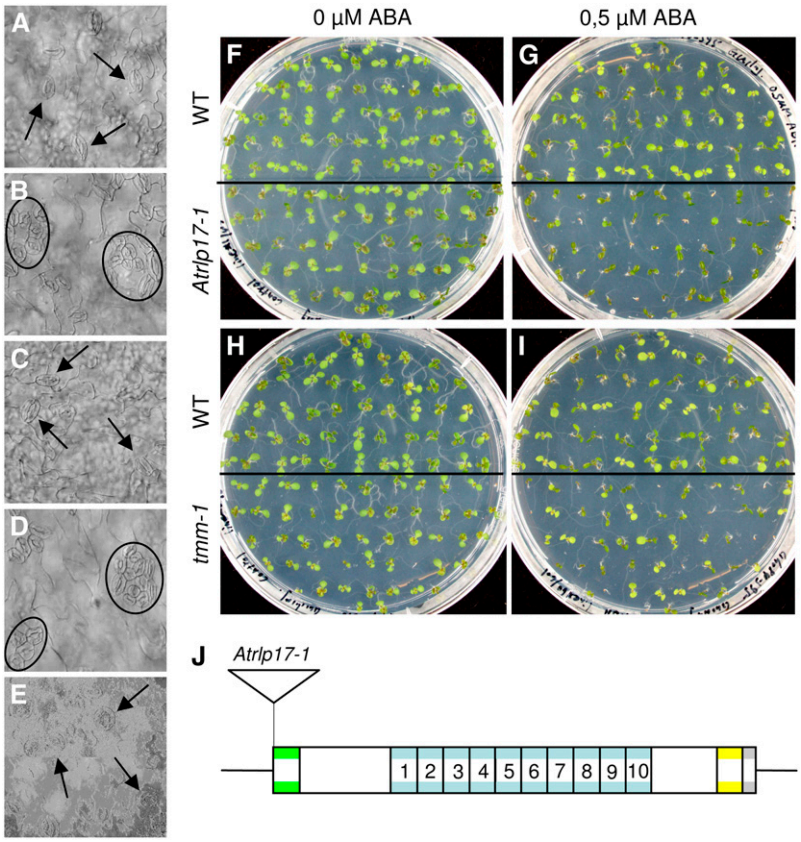

Figure 2. Characterization of the *Atrlp17-1* mutant allele. A to E, Comparison of stomata distribution of wild-type (A and C) with the *Atrlp17-1* mutant (B), *tmm-1* mutant (D), and the *Atrlp17-1* mutant after complementation with a wild-type *TMM* allele (E). The arrows indicate single stomata, while the circles indicate stomatal clusters. F to I, Comparison of ABA response of wild-type (top half of the plate) with *Atrlp17-1* (F and G; bottom half of the plate) or *tmm-1* (H and I; bottom half of the plate) in the absence (F and H) and presence (G and I) of ABA. J, Location of the T-DNA insertion in *Atrlp17-1*.

CLV2 mutants (Fig. 3). Plants from the *Atrlp10-1* T-DNA insertion line grow slower, develop more rosette leaves and shorter stems, and flower at a later stage than wild-type plants and the *clv2-3* mutant (Fig. 3, I–M). During flowering, the meristem of the main inflorescence stops producing flowers for a short period, upon which flowering is resumed (Fig. 3, A, B, and G). However, side stems do not show this temporary termination of the flower meristem. Linkage analysis in a segregating population has demonstrated that the temporary termination of flowering phenotype is linked to a homozygous T-DNA knockout in *Atrlp10-1*. Moreover, complementation of *Atrlp10-1* with the wild-type *CLV2* allele restored all *clv2* mutant phenotypes (Fig. 3, C and L–N).

Conditional Phenotypic Alterations of *AtRLP* Gene T-DNA Insertion Mutants

We tested the collection of T-DNA lines for altered conditional developmental phenotypes, including gravitropism, response to darkness or treatment with different hormones, and a CLV3-like peptide ligand (Supplemental Table S3). For most of the treatments, no consistent differential responsiveness within the collection of *AtRLP* gene knockout lines was observed (data not shown). The only treatment that resulted in a reliable phenotype was a treatment with the plant hormone ABA. In addition to the previously described stomatal clustering phenotype, *tmm-1* and *Atrlp17-1* that both carry a mutation in the *AtRLP* gene *TMM* displayed decreased sensitivity to ABA. Although seedlings of nontreated *Atrlp17-1* and *tmm-1* mutants were phenotypically indistinguishable from control plants (Fig. 2, F and H), exogenous application of ABA induced chlorosis in control plants but not in mutants and reduced the growth of *Atrlp17-1* and *tmm-1* mutants (Fig. 2, G and I) in comparison to the respective control plants. These results indicate that TMM plays a role in ABA-induced chlorosis and growth reduction in Arabidopsis.

Assessment of the Roles of *AtRLP* Genes in Plant Defense

To determine whether *AtRLP* genes play a role in the perception and signaling of abiotic stress signals, we have tested the sensitivity of the collection of T-DNA insertion lines for several abiotic stress inducers. These included inducers of salt stress, osmotic stress, drought stress, reactive oxygen stress, and heavy metal stress (Supplemental Table S3). No consistent phenotypic alterations were observed for any of these abiotic stress stimuli within the collection of T-DNA mutant lines in comparison to wild-type plants.

We have also investigated the possible roles of *AtRLP* genes in the recognition of plant pathogens. The collection of T-DNA insertion lines was assessed for altered phenotypic responses upon pathogen chal-

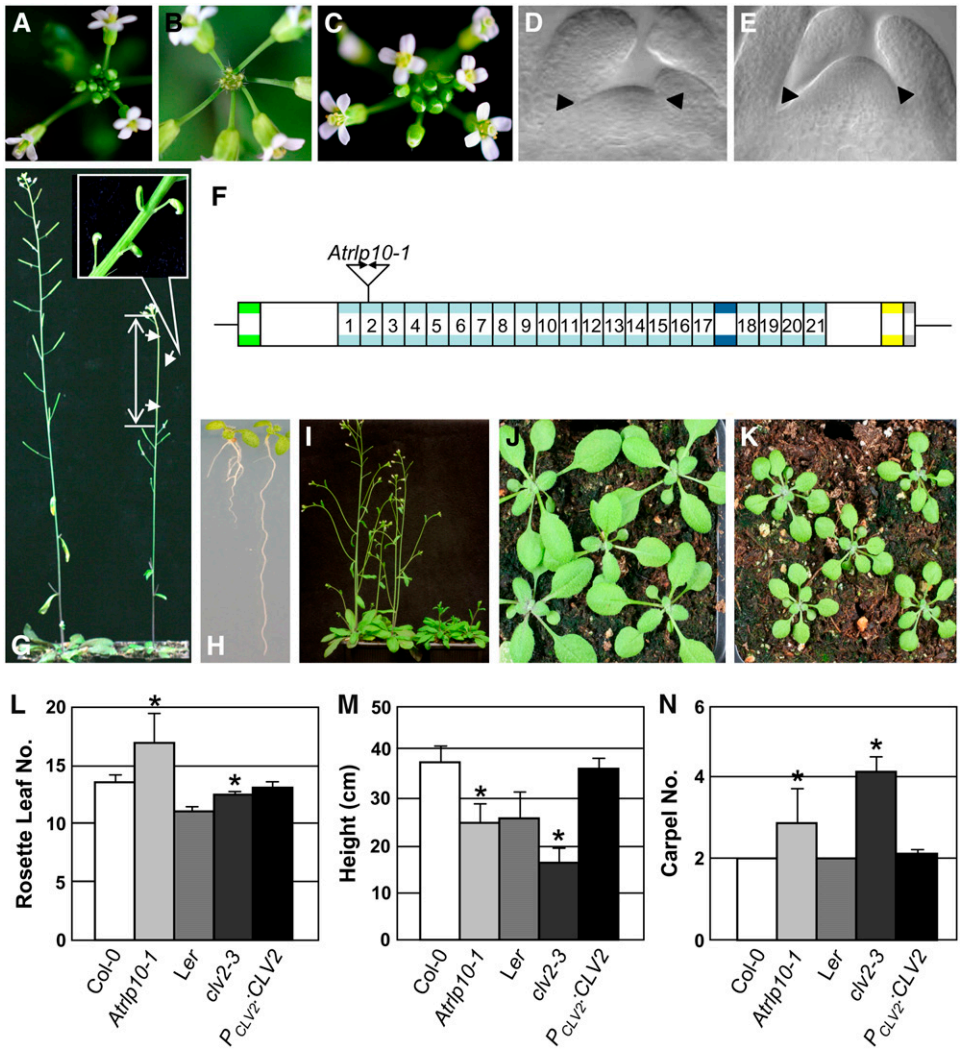

Figure 3. Characterization of the *Atrlp10-1* mutant allele. A, Wild-type inflorescence meristem. B, *Atrlp10-1* inflorescence meristem. C, *Atrlp10-1* inflorescence meristem upon complementation with a wild-type *CLV2* allele. D and E, Cleared shoot meristem of wild type (D) and *Atrlp10-1* (E). Arrowheads indicate meristem borders. F, Location of T-DNA insertion in *Atrlp10* (*CLV2*). G, Comparison of inflorescence development of wild type (left) with *Atrlp10-1* mutant (right). The zoom-in picture indicated no siliques were developed because of the temporary termination of inflorescence meristem of *Atrlp10-1* mutant. H, The 8-d, wild-type seedling (left) showed a short root phenotype, while *Atrlp10-1* (right) shows no effect with 10 μM CLV3p treatment. I, Comparison of 4-week-old plants of wild type (left) with *Atrlp10-1* mutant (right). J and K, Comparison of 2-week-old plants of wild type (J) with *Atrlp10-1* mutant (K). L to N, The mean rosette leaf number (L), height of the primary stem (M), and carpel number (N) of wild types, *clv2-3*, *Atrlp10-1*, and *Atrlp10-1* upon complementation with a wild-type *CLV2* allele. Asterisks indicate significant differences ($P < 0.01$) compared to the respective wild types.

lenge with a diverse range of host-adapted and non-adapted necrotrophic or biotrophic pathogens (Thomma et al., 2001). Nonadapted pathogens are pathogenic on other hosts but normally unable to colonize Arabidopsis. The bacterial pathogens *Pectobacterium atrosepticum*, *P. syringae* pv *tomato* (*Pst*) DC3000, and *Xanthomonas campestris* pv *campestris*; the fungal pathogens *Alternaria brassicicola*, *Botrytis cinerea*, *Cladosporium cucumerinum*, *C. fulvum*, *Colletotrichum destructivum*, *Oidium neolycopersici*, *Plectosphaerella cucumerina*, *Sclerotinia sclerotiorum*, and *Verticillium dahliae*; and the oomycetes *Phytophthora infestans* and *Hyaloperonospora parasitica* were among the pathogens tested (Supplemental Tables S3 and S4). Remarkably, none of the T-DNA insertion lines showed a significant phenotypic alteration in their sensitivity toward these pathogens.

Examination of nonhost interactions was extended using the nonpathogenic bean pathogen *Psp* strain 1448A that is unable to colonize wild-type Col-0 due to changes to the challenged plant cell wall rather than a hypersensitive response (Soylu et al., 2005; de Torres et al., 2006). Colonization by *Psp* 1448A is known to be enhanced in Col-0 *fls2* mutants that lack the ability to perceive flagellin, irrespective of whether inocula are applied to the leaf surface or infiltrated directly into the mesophyll (Zipfel et al., 2004; de Torres et al., 2006). The response of *AtRLP* T-DNA insertion lines to infiltration with bacterial suspensions was examined, and symptom development was compared with both wild-type and *fls2* mutant plants in each set of experiments. We initially recorded the development of yellowing and patchy collapse of infiltrated tissues using an incremental seven-point scoring system. Lines revealing differences in reaction compared with the wild-type Col-0 in the first experiment were further assessed by repeated tests, including measurement of bacterial multiplication. The mutant *Atrlp30-1* recorded consistently enhanced symptom development and more bacterial multiplication with *Psp* 1448A (Fig. 4, A–C). Subsequently, additional insertion mutants in *AtRLP30* recovered from SALK stocks were likewise examined for their reaction to *Psp* 1448A (Fig. 4, D and H; Table II). In all cases, enhanced symptom

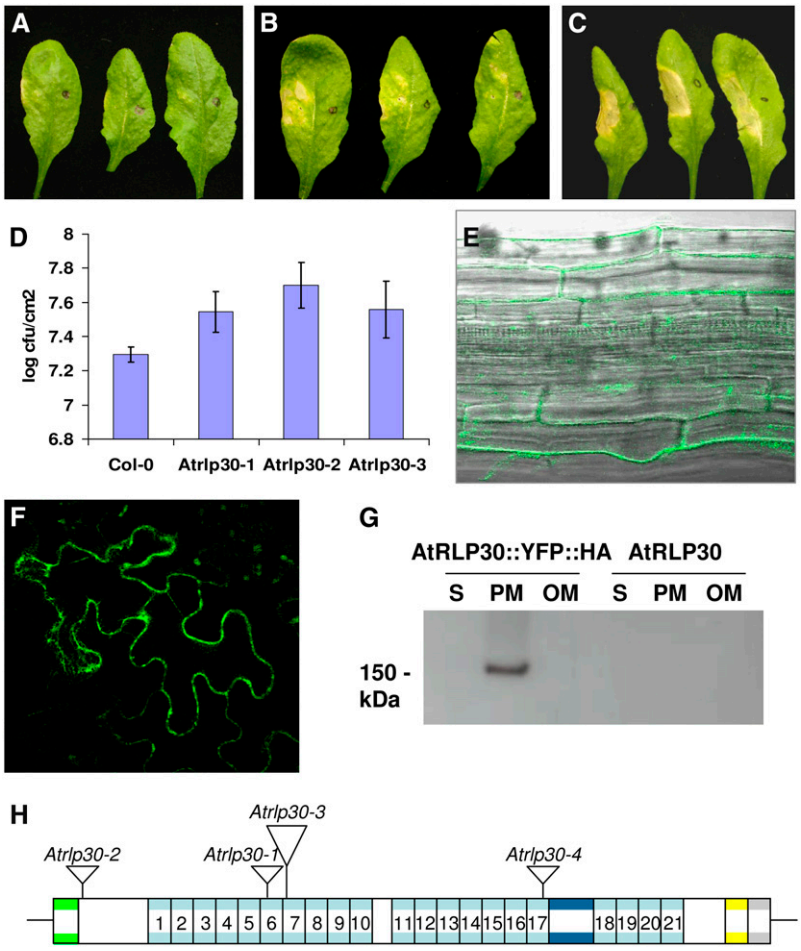

Figure 4. *AtRLP30* is involved in bacterial resistance and localized at the plasma membrane. A to C, Symptom development in Arabidopsis leaves 4 d after inoculation with *Psp*. Areas in half leaves of Col-0 (A), *RLP30-1* (B), and Col-0 *fls2* (C) were syringe inoculated after wounding. Full details of symptom scores are recorded in Table II. D, Comparative analysis of the multiplication of *Psp* 1448A in Col-0 and *Atrlp30* mutant plants. Infiltrated leaves were examined 3 d after inoculation; results are means from four replicates with SES. Statistical analysis using Student's *t* tests showed significantly higher numbers of bacteria in the mutants ($P = 0.047$, 0.014, and 0.088 for *Atrlp30-1*, *-2*, and *-3*, respectively). E to G, Localization of GFP-tagged AtRLP30 in leaf epidermis and petiole tissue as determined using confocal microscopy (E and F) and western blotting with an antibody directed against the HA tag (G). H, Locations of the T-DNA insertions in *AtRLP30*.

development was recorded (Table II) that was associated with the recovery of higher mean numbers of bacteria from infiltrated tissue (Fig. 4D). Student's *t* tests indicated that all of the mutants allowed significantly higher multiplication than Col-0 ($P = 0.05$, 0.01, and 0.08 for *Atrlp30-1*, *Atrlp30-2*, and *Atrlp30-3*, respectively). In all cases, the enhanced symptom development in *AtRLP30* T-DNA mutant lines was lower than observed in the Col-0 *fls2* mutant (Fig. 4, A–C; Table II). Similar as for *Atrlp30* mutants, enhanced susceptibility toward *Psp* 1448A was recorded for *Atrlp18-1* mutants. However, we were unable to further confirm the phenotype due to absence of additional lines with T-DNA insertions in *At2g15040*.

Examination of the enhanced susceptibility phenotype of *Atrlp30* mutants was extended by examining *Pst* strains that carry the avirulence genes *AvrRpm1*, *AvrRpt2*, *AvrRps4*, *AvrPto*, and *AvrPtoB*, and also *hrpA* and *hrcC* mutants of *Pst*, a coronatine-deficient *Pst* mutant, and the nonadapted strain *P. syringae* pv *tabaci* (Supplemental Table S3). However, *Atrlp30* mutants did not display enhanced susceptibility to any of these bacterial strains.

Because of its potential role in basal defense, we examined the subcellular localization of the AtRLP30 protein in Arabidopsis. Transgenic plants expressing C-terminal GFP-tagged AtRLP30 were generated and examined by confocal microscopy. A clear localization of GFP-tagged AtRLP30 to the plasma membrane was, as predicted, observed in the leaf epidermis (Fig. 4F) and petiole tissue (Fig. 4E), which could also be confirmed by western analysis using an antibody directed against the hemagglutinin (HA) tag (Fig. 4G).

The enhanced susceptibility of the *Atrlp30* and *Atrlp18-1* T-DNA insertion mutants to *Psp* 1448A could be explained by an altered responsiveness to the pathogen-associated molecular pattern (PAMP) flagellin. Examination of expression data showed that *AtRLP30* is induced by various PAMPs, including flg22 (Supplemental Fig. S3). We therefore compared the effect of the flg22 flagellin peptide derived from *Psp* 1448A on the seedling growth of Col-0 and the *Atrlp30-1* T-DNA insertion mutant, but no differences were observed (Supplemental Fig. S3). The reduced basal defense observed in the *AtRLP30* mutant was therefore through a route other than flagellin perception. The analysis of response to flg22 was extended to the whole collection of *AtRLP* T-DNA insertion mutants. In no case was any significant alteration in the inhibition of seedling growth observed (Supplemental

Table II. *Symptom development in leaves of Col-0 and mutant lines after syringe inoculation with Psp 1448A*

DPI, Days postinoculation.

Plant	DPI	Frequency of Lesion Type[a]								Mean Score (SD)[b]
		0	1	2	3	4	5	6	7	
Col-0	4	4	5	15						1.46 (0.8)
	6	3	2	9	8	2				2.29 (1.0)
Atrlp30-1	4	1	2	9	2	10				2.75 (1.2)*
	6		5	5	6	7	1			3.75 (1.2)*
Atrlp30-3	4	1	3	11	3	6				2.42 (1.1)*
	6		2	2	7	7	6			3.54 (1.2)*
Atrlp30-4	4	2	2	7	6	7				2.58 (1.2)*
	6		1	3	4	7	9			3.83 (1.2)*
Col-0 *fls2*	4			2	4	9	7	2		4.13 (1.0)*
	6				3	3	8	6	4	5.21 (1.3)*

[a]Three half leaves on eight plants were infiltrated with bacteria at OD_{600} 0.25 (approximately 2×10^8 cells mL^{-1}). Symptom development was scored after 4 and 6 d and sites assigned to each progressive category: 0, no symptoms; 1, very pale yellowing; 2, pale yellowing; 3, yellowing over most of the area infiltrated; 4, pale yellowing with patchy collapse; 5, yellow with patchy collapse; 6, collapse of more than 50% of infiltration site; and 7, collapse of all the infiltrated area. Lack of a number means no sites in the category. [b]Asterisks indicate significant differences ($P < 0.1$) compared to Col-0 at the respective time points.

Table S5). Similarly, none of the *Atrlp* mutant lines had a significant alteration in its response to the necrosis-inducing elicitor protein from *B. cinerea*, BcNEP1 (Schouten et al., 2008), compared to the controls.

Mining of *AtRLP* Expression Data to Uncover Additional *AtRLP*-Regulated Biological Processes

In our unbiased screenings, few novel biological roles have been uncovered for *AtRLP* genes. To gain additional insight into the possible biological processes in which *AtRLP* genes are involved, the Genevestigator online search tool Meta-Analyzer (Zimmermann et al., 2004) was used (Supplemental Fig. S2). This analysis revealed that the expression of the *AtRLP* genes in the context of different organs, growth stages, and stress responses is very diverse. Most *AtRLP* genes are expressed in many organs and developmental stages. *AtRLP4*, which was predicted as a putative developmental ortholog (Fritz-Laylin et al., 2005), is ubiquitously and highly expressed across almost all the developmental stages and organs, confirming a potential basic function in plant development (Supplemental Figs. S1 and S2). However, the development of the *Atrlp4-1* mutant is indistinguishable from that of wild-type plants. Some *AtRLP* genes are specifically expressed in only one or a few organs, such as *AtRLP5*, *AtRLP8*, *AtRLP11*, *AtRLP45*, and *AtRLP48* that are mainly expressed in pollen (Supplemental Fig. S2), suggesting they may play a role at the reproductive stage. However, no defective pollen phenotypes were observed for mutants in those respective genes. The stress response expression data upon challenge with pests and pathogens, hormones, and abiotic stress factors (Supplemental Fig. S2) show differential expression patterns for all *AtRLP* genes. Strikingly, *AtRLP48* is highly induced only upon hormone treatment, and for two hormone treatments (ABA and zeatin), *AtRLP48* is the only *AtRLP* gene induced. Nevertheless, *Atrlp48-1* showed no phenotype upon treatment with these hormones (data not shown).

As many as 25 *AtRLP* genes (*AtRLP2–4*, *7*, *13*, *19*, *20*, *22*, *23*, *26*, *28*, *34–38*, *40–43*, *46*, *47*, *50*, *52*, and *54*) are predominantly expressed in senescent leaves (Supplemental Fig. S2). Of these, five AtRLP-encoding genes (*AtRLP7*, *20*, *28*, *36*, and *42*) are almost exclusively induced in senescent leaves (Supplemental Fig. S2), suggesting a possible function in senescence-related processes. Therefore, we tested whether the 25 *AtRLP* genes are involved in senescence-related processes by subjecting leaves of the corresponding mutants to submergence in ABA. Most of the mutants did not show any altered phenotypes. However, three independent T-DNA insertion lines (Salk_024020, SM_3_20242, and SM_3_38956) of *AtRLP41* displayed enhanced sensitivity upon exogenous application of 100 μM ABA, because the mutant leaves were bleached while wild-type leaves remained green (Fig. 5A). Therefore, our results indicate that *AtRLP41* plays a role in ABA responses.

Previously, *AtRLP51* was reported to be locally induced in roots by the nonpathogenic, root-colonizing rhizobacterium *Pseudomonas fluorescens* WCS417r (Verhagen et al., 2004). This bacterium activates induced systemic resistance (ISR) against a broad range of pathogens (Pieterse et al., 1996). To investigate the role of *AtRLP51* in activation of ISR, we tested the two T-DNA insertion mutants *Atrlp51-1* and *Atrlp51-2* for their ability to express ISR upon treatment with *P. fluorescens* WCS417r. After treatment, plants were inoculated with *Pst* DC3000 or with *B. cinerea*. While wild-type and mutant plants grown in noninfested control soil showed full susceptibility, both wild type and the mutants developed similar levels of ISR toward these pathogens in soil infested with *P. fluorescens*, indicating that *AtRLP51* is not involved in ISR (data not shown).

DISCUSSION

We have undertaken a reverse genetic approach to genome-wide study the role of *RLP* genes in Arabidopsis. Previously, a total of 56 *AtRLP* genes have been identified (Fritz-Laylin et al., 2005). In this study, we identified one additional putative *AtRLP* gene, *AtRLP5*, which corresponds to At1g34290. Although this gene carries only two eLRRs, it complies with the canonical RLP domain composition. Moreover, it has been noted that the number of LRR units of resistance genes and resistance gene analogs can be highly var-

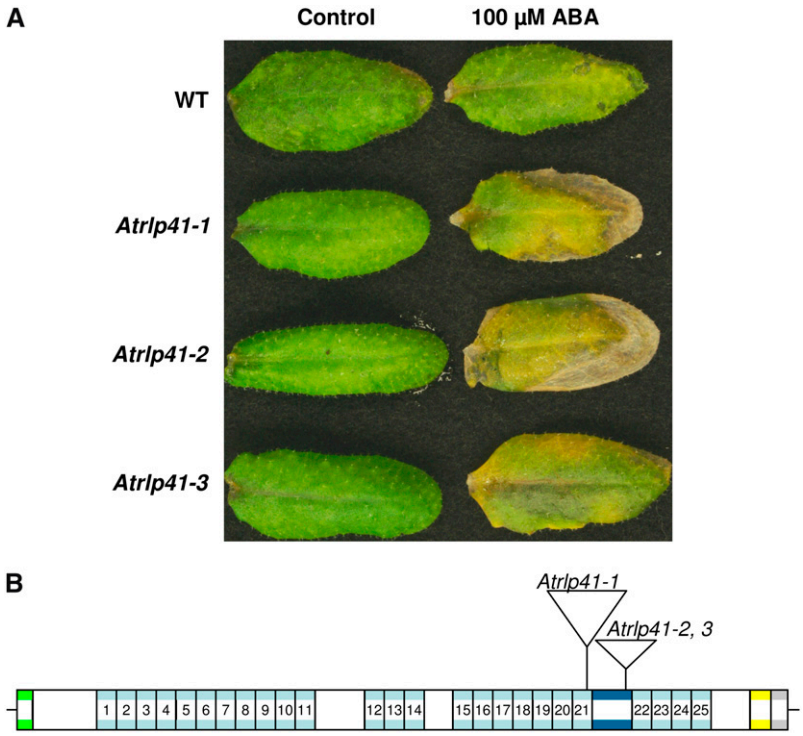

Figure 5. Characterization of the *Atrlp41* mutant alleles. A, Comparison of the leaf phenotype of wild type with mutants *Atrlp41-1*, *Atrlp41-2*, and *Atrlp41-3* after exogenous application of ABA (right). B, The location of T-DNA in *Atrlp41-1*, *Atrlp41-2*, and *Atrlp41-3*.

iable, ranging from one to over two dozen, which is likely to be caused by illegitimate recombination (Wicker et al., 2007). We assembled a genome-wide collection of T-DNA knockout mutants that comprises at least one insertion mutant for 56 of the 57 *AtRLP* genes. We could not obtain any insertion line for just one of the *RLP* genes, *AtRLP19*, which may indicate that insertions in this specific *AtRLP* gene cause lethality. In total, 77 homozygous insertion lines in *AtRLP* genes have been collected that have all been assessed for phenotypic alterations in plant growth and development and for altered responsiveness to various external stimuli, including abiotic stress triggers and microbial pathogens. Previously, biological roles have been assigned to only two *AtRLP* genes, *CLV2* and *TMM* (Jeong et al., 1999; Nadeau and Sack, 2002), while the biological functions of the remaining 55 *AtRLP* genes have remained elusive so far.

In this study, a number of additional novel phenotypes were found for insertion mutants in the *CLV2* and *TMM* genes. Previous studies have demonstrated that mutations in any of the three *CLV* genes result in enlargement of meristems and increased floral organ numbers (Clark et al., 1993, 1995). Our *CLV2* T-DNA insertion allele (*Atrlp10-1*) was found to grow slower, develop more rosette leaves and shorter stems, and develop flowers at a later stage than wild-type plants or *clv2-3* mutants. Furthermore, the meristem of the main inflorescence was found to terminate flowering for a short period, upon which flowering resumed, resulting in an irregular distribution of siliques over the main stem. These novel phenotypes were found to be linked to the T-DNA insertion in *CLV2* and may be attributed to the genetic background of the mutation, as the T-DNA insertion is a mutant of the Col-0 ecotype, while all other previously described *clv2* mutants are backcrossed into the Landsberg *erecta* (L*er*) ecotype (Kayes and Clark, 1998). The progeny of crosses between *Atrlp10-1* and L*er* wild-type plants developed a strong carpel phenotype that is comparable to *clv2* alleles in the L*er* ecotype: more rosette leaves and reduced height without transient termination of the main inflorescence (G. Wang, unpublished data). This suggests that the transient termination of the main inflorescence in *Atrlp10-1* is most likely due to interplay within the genetic background of Col-0.

Previously, *TMM* has been shown to control the initiation of stomatal precursor cells and determine the orientation of the asymmetric divisions that pattern stomata (Geisler et al., 2000; Nadeau and Sack, 2002). In our *TMM* T-DNA insertion mutant (*Atrlp17-1*), we also observed the typical stomatal clustering phenotype. In addition, we found that mutations in *TMM* also displayed altered sensitivity to ABA. Growth of the *TMM* mutants was reduced upon exogenous application of ABA, while the induced chlorosis that is observed in control plants after ABA treatment was not observed. It has long been known that during early stages of drought, plant roots produce ABA that is transported with the transpiration stream and acts as a physiological signal to close stomata. The actual closure is established by an increase of the Ca^{2+} concentration in the guard cell cytoplasm (Schroeder and Hagiwara, 1989). At present, it is not known how *TMM* regulates stomatal distribution, but ABA sensitivity might be a crucial factor in this process. Apart

from *TMM*, a visible altered phenotype upon ABA treatment could be identified for *AtRLP41*, because the corresponding mutants *Atrlp41-1* to *Atrlp41-3* showed enhanced sensitivity to exogenous application of ABA. Nevertheless, for these mutants no abnormalities in stomatal patterning could be observed. *AtRLP41* appeared to be highly induced during plant senescence, and, because ABA is known to be able to act as an inducer of senescence, it is tempting to speculate that *AtRLP41* is involved in ABA-induced senescence responses, although *Atrlp41* mutants did not show any phenotypic alterations at this stage. However, ABA also plays important roles in other processes, including seed development and dormancy (Christmann et al., 2006), which might explain why expression at senescence stages has been reported. Although ABA receptors have not been identified yet, it has been demonstrated that an RLK called RPK1 is involved in early ABA perception in Arabidopsis (Osakabe et al., 2005). Reminiscent to the situation as occurs with the RLK CLV1 that interacts with the RLP CLV2, RPK1 may interact with TMM1 or AtRLP41 to constitute an ABA receptor complex.

Interestingly, it was recently shown that TMM negatively regulates three RLKs during the process of stomatal differentiation, one of which is ERECTA that also controls organ size and shape (Torii et al., 1996; Shpak et al., 2005). In addition, it was recently found that *ERECTA* also regulates plant transpiration efficiency, as *ERECTA* was found to modulate stomatal density through a role in epidermal pavement cell expansion (Masle et al., 2005). Possibly, TMM functions as an anchor protein for multiple RLKs in different signaling processes. A similar situation has recently been demonstrated for the RLK protein BAK1/SERK3 that not only interacts with the RLK BRI1 to modulate brassinosteroid signaling and thus regulate brassinosteroid-dependent growth (Li et al., 2002; Russinova et al., 2004) but also interacts with the RLK FLS2 that acts as a PAMP receptor for bacterial flagellin and functions in innate immunity in a brassinosteroid-independent manner (Chinchilla et al., 2007; Heese et al., 2007). It is anticipated that BAK1 interacts with additional innate immune receptors, because it also regulates full responses to PAMPs that are not related to flagellin, the containment of microbial infection-induced cell death, and restriction of various bacterial, fungal, and oomycete infections (Chinchilla et al., 2007; Heese et al., 2007; Kemmerling et al., 2007). The participation of specific receptor proteins in different receptor complexes may explain why some of these receptors play roles in processes as diverse as plant development and pathogen defense. This is not only the case for BAK1 but also for ERECTA that, in addition to development (Torii et al., 1996; Masle et al., 2005; Shpak et al., 2005), also plays a role in defense (Godiard et al., 2003; Llorente et al., 2005).

Remarkably, among the genome-wide collection of *AtRLP* T-DNA insertion mutants, visibly altered phenotypes were observed for only the four genes *CLV2*, *TMM*, *AtRLP41*, and *AtRLP30*, even though a wide range of developmental stages and treatments were tested. In other plant species, by far most *RLP* genes have been implicated in mediating microbial perception, mostly as pathogen resistance genes (Kruijt et al., 2005). In Arabidopsis, *AtRLP52* has been implicated in resistance against the powdery mildew pathogen *E. cichoracearum* (Ramonell et al., 2005). Interestingly, it was observed that this specific AtRLP is also required for full resistance against the barley (*Hordeum vulgare*) pathogen *Blumeria graminis* f. sp. *hordei* (J. Mansfield, unpublished data). However, in this study, it is rather surprising that only two of the T-DNA insertion lines in the *AtRLP* genes, *AtRLP18* and *AtRLP30*, displayed altered susceptibility upon pathogen challenge. Four independent mutations in *AtRLP30* were found to affect Arabidopsis nonhost defense against the nonadapted bean (*Phaseolus vulgaris*) pathogen *Psp*, although the mutants were not as susceptible as *fls2* mutants defective in the perception of bacterial flagellin. This suggests that, rather than acting as a true resistance gene like all other *RLP*s that have been characterized in plant defense, both AtRLP18 and AtRLP30 act as components of basal defense. Interestingly, defense against another nonadapted *P. syringae* strain (pv *tabaci*) was not compromised, while defense against weakly pathogenic *Pst* strains (*hrpA*, *hcrC*, and coronatine mutants) also appeared to be intact. In tomato, the *RLP* genes *Ve1* and *Ve2* have been implicated in resistance against race 1 strains of the vascular pathogen *V. dahliae* (Kawchuk et al., 2001), which also is a pathogen of Arabidopsis (Fradin and Thomma., 2006). Nevertheless, none of the *AtRLP* insertion lines was found to display altered *V. dahliae* susceptibility. Based on sequence comparison and bioinformatic analysis, it has been suggested that the vast majority of the *AtRLP* genes were likely to act as disease resistance genes. Despite screening a broad spectrum of pathogens with different colonization and feeding styles, we have so far not been able to support this hypothesis. Possibly, this is the consequence of not having used the correct pathogen strains against which these genes are active. Alternatively, the *AtRLP* genes may not act as race-specific disease resistance genes but rather play a role in nonhost resistance or basal host defense. In such cases, the array of potential microbial targets may be dramatically increased and the response to more microbes or even insects and nematodes should be tested (Stout et al., 2006).

The lack of identification of biological functions for *AtRLP* genes may also be explained by functional redundancy, a phenomenon that typically obscures studies employing reverse genetics strategies, as has been described for MADS-box transcription factors (Pařenicová et al., 2003) and *RLK* gene family members (Albrecht et al., 2005; DeYoung et al., 2006; Hord et al., 2006). It has been suggested that CLV1 and CLV2 heterodimerize to form a receptor complex for the secreted CLV3 signaling peptide (Jeong et al., 1999; Ogawa et al., 2008). However, when compared to *clv1*

and *clv3* alleles, *clv2* mutants display relatively weak phenotypes, because fasciation in *clv2* mutants is rarely observed and only under short-day growth conditions (Kayes and Clark, 1998). This may suggest that the role of CLV2 is indeed redundant, although the finding that CLV2, but not CLV1, can perceive the conserved CLE motif of CLV3-like peptides argues against this hypothesis (Fiers et al., 2005). Current strategies employ RNA interference experiments to interfere with the expression of multiple *AtRLP* genes at the same time and thus possibly overcome functional redundancy among *AtRLP* genes. The RNA interference lines that are silenced for multiple *AtRLP* genes can be screened with the various abiotic and biotic stress factors to find biological roles for these *AtRLP* genes.

MATERIALS AND METHODS

Bioinformatic Analysis

To investigate the structure of *AtRLP* genes, BLAST queries were performed using Arabidopsis (*Arabidopsis thaliana*) CLV2 and TMM and tomato (*Solanum lycopersicum*) Cf-9 predicted protein sequences to search translated sequences from the Arabidopsis genome. SMART (http://smart.embl-heidelberg.de), PFAM (http://pfam.janelia.org), SignalP (http://www.cbs.dtu.dk/services/SignalP), and TMHMM (http://www.cbs.dtu.dk/services/TMHMM) were used for domain predictions. The exon/intron boundaries were investigated using GenScan (http://genes.mit.edu/GENSCAN.html), refined using SeqViewer at The Arabidopsis Information Resource (www.arabidopsis.org), and visualized using Jellyfish software (Riethof and Balakrishnan, 2001).

Identification and Analysis of T-DNA Insertion Mutants

The database at SIGnAL (Alonso et al., 2003; http://signal.salk.edu) was searched to identify putative T-DNA insertion mutants, the available lines of interest of which were obtained from the Nottingham Arabidopsis Stock Center (NASC; http://www.arabidopsis.info), GABI-Kat (Rosso et al., 2003; http://www.gabi-kat.de/), or Genoplante FLAGdb/FST (Balzergue et al., 2001; http://urgi.infobiogen.fr). Correct insertion of the T-DNA in these lines was determined with PCR. Genomic DNA was isolated from individual plants that belong to the respective T-DNA insertion lines and used in two separate PCR reactions with different primer sets (Supplemental Table S2). One contained a gene-specific primer and a T-DNA-specific primer to check for the presence of the insertion, and the second PCR contained two gene-specific primers spanning the proposed insertion site to check for nondisrupted alleles. Plants for which the PCR with a gene-specific primer and a T-DNA-specific primer yielded a product, while the PCR with the two gene-specific primers did not yield a product, were considered homozygous insertion lines, which was confirmed in plants from the subsequent generation.

Plant Growth Conditions

Arabidopsis plants of the ecotypes Col-0, Wassilewskija, and L*er* were used. Soil-grown plants were cultured either in a growth chamber at 22°C, 72% relative humidity, and usually a 16-h photoperiod, or in a greenhouse at 21°C during the 16-h day period and 19°C during the night period at 72% relative humidity. In the greenhouse, supplemental light (100 Wm^{-2}) was used when the sunlight influx intensity was below 150 Wm^{-2}.

For in vitro growth of Arabidopsis, seeds were surface sterilized and sown on Murashige and Skoog (MS) medium (Duchefa) solidified with 1.5% plant agar (Duchefa). After sowing, the plates were incubated at 4°C in the dark for 3 d and subsequently transferred to the growth chamber.

Phenotypic Evaluations of Plant Growth and Development

For phenotypic evaluations of plant growth and development, Arabidopsis plants were grown on half-strength MS medium supplemented with 1% Suc and 0.5 g/L MES, pH 5.8. After 2 weeks, plants were transferred to soil for further observations. To assess seed morphology, siliques from the primary inflorescences were screened for seed abortion using a dissection microscope (Tzafrir et al., 2004). Seeds at different developmental stages were mounted in clearing solution (Sabatini et al., 1999), and cleared samples were observed using a Nikon optiphot microscope equipped with Normarski optics. To score vascular patterning and stomatal distribution, cotyledon and rosette leaves were cleared by immersion in ethanol:acetic acid (3:1), subsequently rinsed in 70% ethanol, and incubated in 100% ethanol at 4°C overnight (Jun et al., 2002). The leaves were observed using a dissecting microscope for vascular patterning and Normaski optics for the stomatal distribution. Finally, root geotropism was studied by growing seedlings on vertically oriented half-strength MS plates that were rotated 90° after 6 d of growth. After 10 h, the bending angle of the root was measured (Sedbrook et al., 2002).

Conditional Phenotype Assays

To assess susceptibility toward abiotic stress, seeds were sown on MS plates amended with NaCl (100 or 150 mM), LiCl (20 or 30 mM), mannitol (150 or 200 mM), or hydrogen peroxide (3.3 or 6.7 mM) and evaluated for aberrant growth. To assay heavy metal resistance, plants were grown vertically on half-strength MS medium amended with 2% (w/v) Suc and 85 μM $CdCl_2$ (Lee et al., 2003).

To test whether *AtRLP* genes are involved in responsiveness to hormones, the sterilized seeds were grown on vertically oriented half-strength MS plates containing different hormones at different concentrations (Supplemental Table S3).

To screen whether *AtRLP* genes are involved into leaf senescence, detached leaves were floated on 3 mM MES [2-(*N*-morpholino)ethanesulfonic acid monohydrate] buffer, pH 5.8, in the presence of 50 μM or 100 μM ABA, 50 μM methyl jasmonate, 5 μM ethylene, or 1 μM epibrassinolide (He et al., 2001).

Pathogen Cultivation

Alternaria brassicicola (strain MUCL20297; Mycotheque Université Catholique de Louvain, Louvain-la-Neuve, Belgium), *Cladosporium cucumerinum*, *Cladosporium fulvum*, *Plectospaerella cucumerina* (Thomma et al., 2000), *Sclerotinia sclerotium* strain ND30, and *Verticillium dahliae* strain ST37.01 were maintained on potato dextrose agar (Oxoid). *Botrytis cinerea* (Brouwer et al., 2003) was grown on half-strength potato dextrose agar amended with 5 g/L agar and 150 g/L blended tomato leaves. *Colletotrichum destructivum* (strain IMI349061; CABI Bioscience) was grown on Mathur's agar (Mathur et al., 1950). All fungal in vitro cultures were grown at 22°C. *Oidium neolycopersisi* (Bai et al., 2005) was maintained on Moneymaker tomato plants in the greenhouse. Two GFP transformants of the oomycete *Phytophthora infestans* strains 14.3 (Dr. Govers, Wageningen University, The Netherlands) and 208M2 (Dr. S. Kamoun, Ohio State University) were maintained on rye-agar at 18°C in the dark. Isolates of *Hyaloperonospora parasitica* were maintained as described (Tör et al., 2002). *Pseudomonas syringae* pv *tomato* DC3000 with or without *avrRpt2*, *avrRpm1*, or *avrRps4* were grown on King's B agar (King et al., 1954) supplemented with the appropriate antibiotics (25 μg/mL rifampicin and 100 μg/mL kanamycin). *Pectobacterium atrosepticum* strain LMG 6669 (Coordinated Collections of Micro-organisms, Ghent, Belgium) was maintained on nutrient agar (Oxoid). *Xanthomonas campestris* pv *campestris* (strain 568) was grown on Kado's medium agar (Kado and Heskett, 1970). All bacterial strains were grown overnight at 28°C.

Pathogen Inoculations

All pathogen (except *V. dahliae* and *H. parasitica*) inoculations were performed using soil-grown plants with fully expanded rosette leaves. Inoculum of all in vitro-cultured fungi (except *S. sclerotiorum*) was prepared as previously described (Broekaert et al., 1990) and used as a suspension of 10^6 conidia/mL in water. Inoculations with *A. brassicicola*, *B. cinerea*, *C. destructivum*, and *P. cucumerina* were performed by placing a 6-μL drop of the conidial suspensions on each expanded leaf (Thomma et al., 1998, 2000; O'Connell et al., 2004; Brouwer et al., 2003). *C. fulvum* and *C. cucumerinum* suspensions were sprayed as a mist on the adaxial sides of the leaves. For *V. dahliae* inoculations, 2-week-old Arabidopsis plants were up-rooted, root tips were cut off, and incubated in the conidial suspension for 1 min. Subsequently, the plants were replanted into fresh soil. For *S. sclerotiorum*, three mycelium plugs from a culture plate were placed in a 300-mL flask containing 100 mL of

potato dextrose broth (Difco) and grown for 3 d at 22°C with 150 rpm. Afterward, the mycelium was homogenized in a blender. Leaves were inoculated by placing a 10-μL drop of mycelium fragments (OD_{600} = 3.5) on each of the fully expanded leaves. For *P. infestans*, a rye-agar plate with 10-d-old mycelium was incubated with sterile water at 4°C for 2 h to release zoospores from zoosporangia. One 5-μL drop of a suspension of 10^5 zoospores/mL in water was placed on each fully expanded leaf. To avoid background fluorescence from superficial growing *P. infestans*, the drops were removed by drying with tissue paper after 36 h. For *Oidium neolycopersici*, 10^5 conidia/mL was used. The inoculation was performed as described by Bai et al. (2005). Inoculations of Arabidopsis seedlings with *H. parasitica* were performed as described (Tör et al., 2002).

For all bacterial inoculations, bacteria were grown overnight at 28°C in the appropriate medium supplemented with the appropriate antibiotics. Strains of *P. syringae* (except *P. syringae* pv *phaseolicola* [*Psp*]) and *P. atrosepticum* were spray inoculated with a bacterial suspension of OD_{600} 0.3 supplemented with 0.05% [v/v] Silwet L-77 (van Meeuwen Chemicals). For *X. campestris*, two different inoculation methods were carried out (Meyer et al., 2005): infiltration of a concentrated bacterial suspension or wound inoculation.

For *Psp* 1448A, three half leaves on eight plants were infiltrated with bacteria at OD_{600} 0.25 (approximately 2×10^8 cells/mL). Symptom development was scored after 4 and 6 d and sites assigned to each progressive category: 0, no symptoms; 1, very pale yellowing; 2, pale yellowing; 3, yellowing over most of the area infiltrated; 4, pale yellowing with patchy collapse; 5, yellow with patchy collapse; 6, collapse of more than 50% of infiltration site; and 7, collapse of all the infiltrated area. Bacterial numbers were recorded as described by de Torres et al. (2006).

For all inoculations, except those with *O. neolycopersici* and *V. dahliae*, plants were kept in boxes with transparent lids at high relative humidity for the remainder of the experiment. As a positive control for the inoculations with *A. brassicicola*, *B. cinerea*, and *P. cucumerina*, *pad3-1* mutant plants were used (Thomma et al., 1999, 2000; Kliebenstein et al., 2005). For *P. infestans*, the *pen2-1* mutant was used (Lipka et al., 2005), while for the *Pseudomonas* strains the genotypes *NahG* and *npr1-1* were used (Thomma et al., 1998). Finally, for *X. campestris* the ecotype Kas was used as positive control (Xu et al., 2008).

To test whether *AtRLP51* is involved in ISR expression, the ISR bioassay was performed as described by Pieterse et al. (1996) except for the challenge inoculation. For *P. syringae* and for *B. cinerea*, the inoculations were performed as mentioned previously. Except for *P. syringae*, a lower concentration of a bacterial suspension of OD_{600} 0.3 five times diluted was used.

Response to Pathogen Elicitors

Flg22-induced seedling growth inhibition assays (Gomez-Gomez et al., 1999) were performed essentially as described (Pfund et al., 2004). After germination of Arabidopsis seeds for 5 d at 22°C, two seedlings were transferred to 750 mL of liquid MS medium in a 25-well plate either with or without 2 mg/L flg22 peptide (sequence, TRLSSGKINSAKDDAAGL). Each treatment was replicated five times. After 2 weeks further growth, the weights of the seedlings were recorded. Wassilewskija-0, Col-0 *fls2* (insensitive to flg22), and Col-0 (susceptible to flg22 growth inhibition) were used as controls in each experiment.

Leaves of Arabidopsis plants were pressure infiltrated with the *B. cinerea* elicitor protein BcNEP1 that was isolated from a *Pichia pastoris* culture heterologously expressing *BcNEP1*. A raw protein extract from culture filtrate containing the BcNEP1 protein was isolated as described (Schouten et al., 2008) and was 10 times diluted in MMA (5 g/L MS salts [Duchefa], 1.9 g/L MES).

Localization of AtRLP30

AtRLP30 is predicted to contain a single exon, which was confirmed by sequencing full-length cDNA from Col-0 amplified using reverse transcription-PCR. The resulting cDNA was cloned into the gateway entry vector pDONR/Zeo using BP clonase (Invitrogen) and subsequently transferred to the gateway-compatible binary vector pEarleyGate101 (Earley et al., 2006) using LR clonase (Invitrogen). This resulted in a plasmid with *AtRLP30* fused to the coding sequence of YFP::HA and expression was driven by the cauliflower mosaic virus 35S promoter. The T-DNA insertion line Salk_122528, homozygous for the insertion in *AtRLP30*, was transformed with this plasmid using the floral dip method (Clough and Bent, 1998). Transgenic plants were selected on soil soaked with 150 mg/L Basta herbicide (glufosinate-ammonium, Bayer CropScience) and confirmed by PCR. Plants were checked for fluorescence using an Olympus IX70 microscope equipped with a Fluroview 300 confocal laser scanning unit. AtRLP30::YFP::HA fluorescence was excited with a 488-nm argon laser and fluorescence was detected between 510 nm and 530 nm.

Supplemental Data

The following materials are available in the online version of this article.

Supplemental Figure S1. cDNA, EST, and Massively Parallel Signature Sequencing expression data for *AtRLP* genes.

Supplemental Figure S2. Expression profile of *AtRLP* genes in various organs and growth stages and upon stress responses.

Supplemental Figure S3. Expression of *AtRLP30* after PAMP treatment.

Supplemental Table S1. Pairwise alignment of AtRLP amino acid sequences.

Supplemental Table S2. Primers used to check for the presence of the predicted T-DNA insertions.

Supplemental Table S3. Conditional phenotype assays for AtRLP mutants.

Supplemental Table S4. Interaction phenotypes of AtRLP mutants with isolates of *H. parasitica*.

Supplemental Table S5. Screening of RLP mutants with flg22 using seedling assays.

ACKNOWLEDGMENTS

We thank Drs. Shiu, Fritz-Laylin, and Yang for valuable discussion. We are grateful to NASC, GABI-Kat, and Genoplante FLAGdb/FST for providing plant materials. We further acknowledge Drs. Rao Uppalapati, Yuling Bai, Francine Govers, Thomas Kroj, Bart Lievens, and Berlin Nelson for providing pathogen strains, and Blaise Alako, Bert Essenstam, Terry Amatulli, Ann Baker, Nina Grabov, and Zhao Zhang for technical assistance.

Received March 20, 2008; accepted April 11, 2008; published April 23, 2008.

LITERATURE CITED

Albrecht C, Russinova E, Hecht V, Baaijens E, De Vries S (2005) The *Arabidopsis thaliana* SOMATIC EMBRYOGENESIS RECEPTOR-LIKE KINASES1 and 2 control male sporogenesis. Plant Cell **17:** 3337–3349

Alonso JM, Stepanova AN, Leisse TJ, Kim CJ, Chen H, Shinn P, Stevenson DK, Zimmerman J, Barajas P, Cheuk R, et al (2003) Genome-wide insertional mutagenesis of *Arabidopsis thaliana.* Science **301:** 653–657

Arabidopsis Genome Initiative (2000) Analysis of the genome sequence of the flowering plant *Arabidopsis thaliana.* Nature **408:** 796–815

Bai YL, van der Hulst R, Bonnema G, Marcel BC, Meijer-Dekens F, Niks RE, Lindhout P (2005) Tomato defense to *Oidium neolycopersici*: dominant *Ol* genes confer isolate-dependent resistance via a different mechanism than recessive *ol-2*. Mol Plant Microbe Interact **18:** 354–362

Balzergue S, Dubreucq B, Chauvin S, Le-Clainche I, Le Boulaire F, De Rose R, Samson F, Biaudet V, Lecharny A, Cruaud C, et al (2001) Improved PCR-walking for large-scale isolation of plant T-DNA borders. Biotechniques **30:** 496–504

Belfanti E, Silfverberg-Dilworth E, Tartarini S, Patocchi A, Barbieri M, Zhu J, Vinatzer BA, Gianfranceschi L, Gessler C, Sansavini S (2004) The *HcrVf2* gene from a wild apple confers scab resistance to a transgenic cultivated variety. Proc Natl Acad Sci USA **101:** 886–890

Bommert P, Satoh-Nagasawa N, Jackson D, Hirano HY (2005) Genetics and evolution of inflorescence and flower development in grasses. Plant Cell Physiol **46:** 69–78

Broekaert WF, Terras FRG, Cammue BPA, Vanderleyden J (1990) An automated quantitative assay for fungal growth inhibition. FEMS Microbiol Lett **69:** 55–59

Brouwer M, Lievens B, Van Hemelrijck W, Van Den Ackerveken G, Cammue BPA, Thomma BPHJ (2003) Quantification of disease pro-

gression of several microbial pathogens on *Arabidopsis thaliana* using real-time fluorescence PCR. FEMS Microbiol Lett **228:** 241–248

Chinchilla D, Zipfel C, Robatzek S, Kemmerling B, Nürnberger T, Jones JDG, Felix G, Boller T (2007) A flagellin-induced complex of the receptor FLS2 and BAK1 initiates plant defence. Nature **448:** 497–500

Christmann A, Moes D, Himmelbach A, Yang Y, Tang Y, Grill E (2006) Integration of abscisic acid signalling into plant responses. Plant Biol **8:** 314–325

Clark SE, Running MP, Meyerowitz EM (1993) *CLAVATA1*, a regulator of meristem and flower development in Arabidopsis. Development **119:** 397–418

Clark SE, Running MP, Meyerowitz EM (1995) *CLAVATA3* is a specific regulator of shoot and floral meristem development affecting the same processes as *CLAVATA1*. Development **121:** 2057–2067

Clark SE, Williams RW, Meyerowitz EM (1997) The *CLAVATA1* gene encodes a putative receptor kinase that controls shoot and floral meristem size in Arabidopsis. Cell **89:** 575–585

Clough SJ, Bent AF (1998) Floral dip: a simplified method for *Agrobacterium*-mediated transformation of *Arabidopsis thaliana*. Plant J **16:** 735–743

de Torres M, Mansfield JW, Grabov N, Brown IR, Ammouneh H, Tsiamis G, Forsyth A, Robatzek S, Grant M, Boch J (2006) *Pseudomonas syringae* effector AvrPtoB suppresses basal defence in Arabidopsis. Plant J **47:** 368–382

DeYoung BJ, Bickle KL, Schrage KJ, Muskett P, Patel K, Clark SE (2006) The CLAVATA1-related BAM1, BAM2 and BAM3 receptor kinase-like proteins are required for meristem function in Arabidopsis. Plant J **45:** 1–16

Diévart A, Clark SE (2004) LRR-containing receptors regulating plant development and defense. Development **131:** 251–261

Dixon MS, Hatzixanthis K, Jones DA, Harrison K, Jones JDG (1998) The tomato *Cf-5* disease resistance gene and six homologs show pronounced allelic variation in leucine-rich repeat copy number. Plant Cell **10:** 1915–1925

Dixon MS, Jones DA, Keddie JS, Thomas CM, Harrison K, Jones JDG (1996) The tomato *Cf-2* disease resistance locus comprises two functional genes encoding leucine-rich repeat proteins. Cell **84:** 451–459

Earley K, Haag JR, Pontes O, Opper K, Juehne T, Song K, Pikaard CS (2006) Gateway-compatible vectors for plant functional genomics and proteomics. Plant J **45:** 616–629

Fiers M, Golemiec E, Xu J, Van Der Geest L, Heidstra R, Stiekema W, Liu CM (2005) The 14-amino acid *CLV3, CLE19,* and *CLE40* peptides trigger consumption of the root meristem in *Arabidopsis* through a *CLAVATA2*-dependent pathway. Plant Cell **17:** 2542–2553

Fradin EF, Thomma BPHJ (2006) Physiology and molecular aspects of *Verticillium* wilt diseases caused by *V. dahliae* and *V. albo-atrum*. Mol Plant Pathol **7:** 71–86

Fritz-Laylin LK, Krishnamurthy N, Tör M, Sjölander KV, Jones JDG (2005) Phylogenomic analysis of the receptor-like proteins of rice and Arabidopsis. Plant Physiol **138:** 611–623

Geisler M, Nadeau J, Sack FD (2000) Oriented asymmetric divisions that generate the stomatal spacing pattern in *Arabidopsis* are disrupted by the *too many mouths* mutation. Plant Cell **12:** 2075–2086

Godiard L, Sauviac L, Torii KU, Grenon O, Mangin B, Grimsley NH, Marco Y (2003) ERECTA, an LRR receptor-like kinase protein controlling development pleiotropically affects resistance to bacterial wilt. Plant J **36:** 353–365

Gómez-Gómez L, Boller T (2000) FLS2: an LRR receptor-like kinase involved in the perception of the bacterial elicitor flagellin in Arabidopsis. Mol Cell **5:** 1003–1011

Gomez-Gomez L, Felix G, Boller T (1999) A single locus determines sensitivity to bacterial flagellin in *Arabidopsis thaliana*. Plant J **18:** 277–284

He Y, Tang W, Swain J, Green A, Jack T, Gan S (2001) Networking senescence-regulating pathways by using Arabidopsis enhancer trap lines. Plant Physiol **126:** 707–716

Heese A, Hann DR, Gimenez-Ibanez S, Jones AM, He K, Li J, Schroeder JI, Peck SC, Rathjen JP (2007) The receptor-like kinase SERK3/BAK1 is a central regulator of innate immunity in plants. Proc Natl Acad Sci USA **104:** 12217–12222

Hord CL, Chen C, Deyoung BJ, Clark SE, Ma H (2006) The BAM1/BAM2 receptor-like kinases are important regulators of *Arabidopsis* early anther development. Plant Cell **18:** 1667–1680

Jeong S, Trotochaud AE, Clark SE (1999) The *Arabidopsis CLAVATA2* gene encodes a receptor-like protein required for the stability of the CLAVATA1 receptor-like kinase. Plant Cell **11:** 1925–1933

Jones DA, Jones JDG (1997) The role of leucine-rich repeat proteins in plant defences. Adv Bot Res **24:** 89–167

Jones DA, Thomas CM, Hammond-Kosack KE, Balint-Kurti PJ, Jones JDG (1994) Isolation of the tomato *Cf-9* gene for resistance to *Cladosporium fulvum* by transposon tagging. Science **266:** 789–793

Joosten MHAJ, de Wit PJGM (1999) The tomato-*Cladosporium fulvum* interaction: a versatile experimental system to study plant-pathogen interactions. Annu Rev Phytopathol **37:** 335–367

Jun JH, Ha CM, Nam HG (2002) Involvement of the *VEP1* gene in vascular strand development in *Arabidopsis thaliana*. Plant Cell Physiol **43:** 323–330

Kado CI, Heskett MG (1970) Selective media for isolation of *Agrobacterium, Corynebacterium, Erwinia, Pseudomonas,* and *Xanthomonas*. Phytopathology **60:** 969–976

Kawchuk LM, Hachey J, Lynch DR, Kulcsar F, Van Rooijen G, Waterer DR, Robertson A, Kokko E, Byers R, Howard RJ, et al (2001) Tomato *Ve* disease resistance genes encode cell surface-like receptors. Proc Natl Acad Sci USA **98:** 6511–6515

Kayes JM, Clark SE (1998) *CLAVATA2*, a regulator of meristem and organ development in Arabidopsis. Development **125:** 3843–3851

Kemmerling B, Schwedt A, Rodriguez P, Mazzotta S, Frank M, Qamar SA, Mengiste T, Betsuyaku S, Parker JE, Mussig C, et al (2007) The BRI1-associated kinase 1, BAK1, has a brassinolide-independent role in plant cell-death control. Curr Biol **17:** 1116–1122

King EO, Ward MK, Raney DE (1954) Two simple media for the demonstration of phycocyanin and fluorescin. J Lab Clin Med **44:** 301–307

Kinoshita T, Caño-Delgado A, Seto H, Hiranuma S, Fujioka S, Yoshida S, Chory J (2005) Binding of brassinosteroids to the extracellular domain of plant receptor kinase BRI1. Nature **433:** 167–171

Kliebenstein DJ, Rowe HC, Denby KJ (2005) Secondary metabolites influence Arabidopsis/*Botrytis* interactions: variation in host production and pathogen sensitivity. Plant J **44:** 25–36

Kobe B, Kajava AV (2001) The leucine-rich repeat as a protein recognition motif. Curr Opin Struct Biol **11:** 725–732

Kruijt M, De Kock MJD, de Wit PJGM (2005) Receptor-like proteins involved in plant disease resistance. Mol Plant Pathol **6:** 85–97

Lee S, Moon JS, Ko TS, Petros D, Goldsbrough PB, Korban SS (2003) Overexpression of *Arabidopsis* phytochelatin synthase paradoxically leads to hypersensitivity to cadmium stress. Plant Physiol **131:** 656–663

Leister D (2004) Tandem and segmental gene duplication and recombination in the evolution of plant disease resistance genes. Trends Genet **20:** 116–122

Li CM, Brown I, Mansfield J, Stevens C, Boureau T, Romantschuk M, Taira S (2002) The Hrp pilus of *Pseudomonas syringae* elongates from its tip and acts as a conduit for translocation of the effector protein HrpZ. EMBO J **21:** 1909–1915

Li J, Chory J (1997) A putative leucine-rich repeat receptor kinase involved in brassinosteroid signal transduction. Cell **90:** 929–938

Li J, Jin H (2007) Regulation of brassinosteroid signaling. Trends Plant Sci **12:** 37–41

Li J, Wen J, Lease KA, Doke JT, Tax FE, Walker JC (2002) BAK1, an Arabidopsis LRR receptor-like protein kinase, interacts with BRI1 and modulates brassinosteroid signaling. Cell **110:** 213–222

Lipka V, Dittgen J, Bednarek P, Bhat R, Wiermer M, Stein M, Landtag J, Brandt W, Rosahl S, Scheel D, et al (2005) Pre- and postinvasion defenses both contribute to nonhost resistance in Arabidopsis. Science **310:** 1180–1183

Llorente F, Alonso-Blanco C, Sanchez-Rodriguez C, Jorda L, Molina A (2005) ERECTA receptor-like kinase and heterotrimeric G protein from Arabidopsis are required for resistance to the necrotrophic fungus *Plectosphaerella cucumerina*. Plant J **43:** 165–180

Masle J, Gilmore SR, Farquhar GD (2005) The *ERECTA* gene regulates plant transpiration efficiency in Arabidopsis. Nature **436:** 866–870

Mathur RS, Barnett HL, Lilly VG (1950) Sporulation of *Colletotrichum lindemuthianum* in culture. Phytopathology **40:** 104–114

Meyer D, Lauber E, Roby D, Arlat M, Kroj T (2005) Optimization of pathogenicity assays to study the *Arabidopsis thaliana-Xanthomonas campestris* pv. *campestris* pathosystem. Mol Plant Pathol **6:** 327–333

Nadeau JA, Sack FD (2002) Control of stomatal distribution on the Arabidopsis leaf surface. Science **296:** 1697–1700

Nürnberger T, Kemmerling B (2006) Receptor protein kinases: pattern recognition receptors in plant immunity. Trends Plant Sci **11:** 519–522

O'Connell R, Herbert C, Sreenivasaprasad S, Khatib M, Esquerre-Tugaye MT, Dumas B (2004) A novel *Arabidopsis-Colletotrichum* pathosystem for

the molecular dissection of plant-fungal interactions. Mol Plant Microbe Interact **17:** 272–282

Ogawa M, Shinohara H, Sakagami Y, Matsubayashi Y (2008) Arabidopsis CLV3 peptide directly binds CLV1 ectodomain. Science **319:** 294

Osakabe Y, Maruyama K, Seki M, Satou M, Shinozaki K, Yamaguchi-Shinozaki K (2005) Leucine-rich repeat receptor-like kinase1 is a key membrane-bound regulator of abscisic acid early signaling in *Arabidopsis*. Plant Cell **17:** 1105–1119

Pařenicová L, de Folter S, Kieffer M, Horner DS, Favalli C, Busscher J, Cook HE, Ingram RM, Kater MM, Davies B, et al (2003) Molecular and phylogenetic analyses of the complete MADS-box transcription factor family in *Arabidopsis*. Plant Cell **15:** 1538–1551

Pfund C, Tans-Kersten J, Dunning FM, Alonso JM, Ecker JR, Allen C, Bent AF (2004) Flagellin is not a major defense elicitor in *Ralstonia solanacearum* cells or extracts applied to *Arabidopsis thaliana*. Mol Plant Microbe Interact **17:** 696–706

Pieterse CMJ, Van Wees SCM, Hoffland E, Van Pelt JA, Van Loon LC (1996) Systemic resistance in *Arabidopsis* induced by biocontrol bacteria is independent of salicylic acid accumulation and pathogenesis-related gene expression. Plant Cell **8:** 1225–1237

Ramonell K, Berrocal-Lobo M, Koh S, Wan JR, Edwards H, Stacey G, Somerville S (2005) Loss-of-function mutations in chitin responsive genes show increased susceptibility to the powdery mildew pathogen *Erysiphe cichoracearum*. Plant Physiol **138:** 1027–1036

Riethof DA, Balakrishnan R (2001) LabVelocity: online tools for life science products, protocols, technical information, MEDLINE searches, and laboratory calculations. Biotechniques **30:** 1310–1315

Rojo E, Sharma VK, Kovaleva V, Raikhel NV, Fletcher JC (2002) CLV3 is localized to the extracellular space, where it activates the *Arabidopsis* CLAVATA stem cell signaling pathway. Plant Cell **14:** 969–977

Ron M, Avni A (2004) The receptor for the fungal elicitor ethylene-inducing xylanase is a member of a resistance-like gene family in tomato. Plant Cell **16:** 1604–1615

Rosso MG, Li Y, Strizhov N, Reiss B, Dekker K, Weisshaar B (2003) An *Arabidopsis thaliana* T-DNA mutagenized population (GABI-Kat) for flanking sequence tag-based reverse genetics. Plant Mol Biol **53:** 247–259

Russinova E, Borst JW, Kwaaitaal M, Cano-Delgado A, Yin Y, Chory J, de Vries SC (2004) Heterodimerization and endocytosis of *Arabidopsis* brassinosteroid receptors BRI1 and AtSERK3 (BAK1). Plant Cell **16:** 3216–3229

Sabatini S, Beis D, Wolkenfelt H, Murfett J, Guilfoyle T, Malamy J, Benfey P, Leyser O, Bechtold N, Weisbeek P, et al (1999) An auxin-dependent distal organizer of pattern and polarity in the Arabidopsis root. Cell **99:** 463–472

Schouten A, van Baarlen P, van Kan JA (2008) Phytotoxic Nep1-like proteins from the necrotrophic fungus *Botrytis cinerea* associate with membranes and the nucleus of plant cells. New Phytol **177:** 493–505

Schroeder JL, Hagiwara S (1989) Cytosolic calcium regulates ion channels in the plasma membrane of *Vicia faba* guard cells. Nature **338:** 427–430

Sedbrook JC, Carroll KL, Hung KF, Masson PH, Somerville CR (2002) The *Arabidopsis* SKU5 gene encodes an extracellular glycosyl phosphatidylinositol-anchored glycoprotein involved in directional root growth. Plant Cell **14:** 1635–1648

Shiu SH, Bleecker AB (2003) Expansion of the receptor-like kinase/Pelle gene family and receptor-like proteins in Arabidopsis. Plant Physiol **132:** 530–543

Shpak ED, McAbee JM, Pillitteri LJ, Torii KU (2005) Stomatal patterning and differentiation by synergistic interactions of receptor kinases. Science **309:** 290–293

Song WY, Wang GL, Chen LL, Kim HS, Pi LY, Holsten T, Gardner J, Wang B, Zhai WX, Zhu LH, et al (1995) A receptor kinase-like protein encoded by the rice disease resistance gene, *Xa21*. Science **270:** 1804–1806

Soylu S, Brown IR, Mansfield JW (2005) Cellular reactions in Arabidopsis following challenge by strains of *Pseudomonas syringae*: from basal resistance to compatibility. Physiol Mol Plant Pathol **66:** 232–243

Stout MJ, Thaler JS, Thomma BPHJ (2006) Plant-mediated interactions between pathogenic microorganisms and herbivorous arthropods. Annu Rev Entomol **51:** 663–689

Taguchi-Shiobara F, Yuan Z, Hake S, Jackson D (2001) The *fasciated ear2* gene encodes a leucine-rich repeat receptor-like protein that regulates shoot meristem proliferation in maize. Genes Dev **15:** 2755–2766

Takken FLW, Thomas CM, Joosten MHAJ, Golstein C, Westerink N, Hille J, Nijkamp HJJ, De Wit PJGM, Jones JDG (1999) A second gene at the tomato *Cf-4* locus confers resistance to *Cladosporium fulvum* through recognition of a novel avirulence determinant. Plant J **20:** 279–288

Thomas CM, Jones DA, Parniske M, Harrison K, Balint-Kurti PJ, Hatzixanthis K, Jones JDG (1997) Characterization of the tomato *Cf-4* gene for resistance to *Cladosporium fulvum* identifies sequences that determine recognitional specificity in Cf-4 and Cf-9. Plant Cell **9:** 2209–2224

Thomma BPHJ, Eggermont K, Broekaert WF, Cammue BPA (2000) Disease development of several fungi on Arabidopsis can be reduced by treatment with methyl jasmonate. Plant Physiol Biochem **38:** 421–427

Thomma BPHJ, Eggermont K, Penninckx IAMA, Mauch-Mani B, Vogelsang R, Cammue BPA, Broekaert WF (1998) Separate jasmonate-dependent and salicylate-dependent defense-response pathways in Arabidopsis are essential for resistance to distinct microbial pathogens. Proc Natl Acad Sci USA **95:** 15107–15111

Thomma BPHJ, Nelissen I, Eggermont K, Broekaert WF (1999) Deficiency in phytoalexin production causes enhanced susceptibility of *Arabidopsis thaliana* to the fungus *Alternaria brassicicola*. Plant J **19:** 163–171

Thomma BPHJ, Penninckx IAMA, Broekaert WF, Cammue BPA (2001) The complexity of disease signaling in Arabidopsis. Curr Opin Immunol **13:** 63–68

Thomma BPHJ, Van Esse HP, Crous PW, de Wit PJGM (2005) *Cladosporium fulvum* (syn. *Passalora fulva*), a highly specialized plant pathogen as a model for functional studies on plant pathogenic Mycosphaerellaceae. Mol Plant Pathol **6:** 379–393

Tör M, Gordon P, Cuzick A, Eulgem T, Sinapidou E, Mert F, Can C, Dangl JL, Holub EB (2002) *Arabidopsis* SGT1b is required for defence signaling conferred by several downy mildew (*Peronospora parasitica*) resistance genes. Plant Cell **14:** 993–1003

Torii KU, Mitsukawa N, Oosumi T, Matsuura Y, Yokoyama R, Whittier RF, Komeda Y (1996) The *Arabidopsis ERECTA* gene encodes a putative receptor protein kinase with extracellular leucine-rich repeats. Plant Cell **8:** 735–746

Trotochaud AE, Hao T, Wu G, Yang Z, Clark SE (1999) The CLAVATA1 receptor-like kinase requires CLAVATA3 for its assembly into a signaling complex that includes KAPP and a Rho-related protein. Plant Cell **11:** 393–406

Tzafrir I, Pena-Muralla R, Dicherman A, Berg M, Rogers R, Hutchens S, Sweeney TC, McElver J, Aux G, Patton D, et al (2004) Identification of genes required for embryo development in Arabidopsis. Plant Physiol **135:** 1206–1220

Verhagen BWM, Glazebrook J, Zhu T, Chang HS, Van Loon LC, Pieterse CMJ (2004) The transcriptome of rhizobacteria-induced systemic resistance in Arabidopsis. Mol Plant Microbe Interact **17:** 895–908

Walker JC, Zhang R (1990) Relationship of a putative receptor protein-kinase from maize to the S-locus glycoproteins of *Brassica*. Nature **345:** 743–746

Wicker T, Yahiaoui N, Keller B (2007) Illegitimate recombination is a major evolutionary mechanism for initiating size variation in plant resistance genes. Plant J **51:** 631–641

Xu RQ, Blanvillain S, Feng JX, Jiang BL, Li XZ, Wei HY, Kroj T, Lauber E, Roby D, Chen B, et al (2008) AvrAC(Xcc8004), a type III effector with a leucine-rich repeat domain from *Xanthomonas campestris* pathovar *campestris* confers avirulence in vascular tissues of *Arabidopsis thaliana* ecotype Col-0. J Bacteriol **190:** 343–355

Yang M, Sack FD (1995) The *too many mouths* and *four lips* mutations affect stomatal production in *Arabidopsis*. Plant Cell **7:** 2227–2239

Zimmermann P, Hirsch-Hoffmann M, Hennig L, Gruissem W (2004) GENEVESTIGATOR. Arabidopsis microarray database and analysis toolbox. Plant Physiol **136:** 2621–2632

Zipfel C, Robatzek S, Navarro L, Oakeley EJ, Jones JDG, Felix G, Boller T (2004) Bacterial disease resistance in Arabidopsis through flagellin perception. Nature **428:** 764–767